

# Understanding Diastereofacial Selection in Carbohydrate-Based Domino Cycloadditions: Semiempirical and DFT Calculations

Martín Avalos, Reyes Babiano, José L. Bravo, Pedro Cintas,\* José L. Jiménez, Juan C. Palacios, and María A. Silva<sup>[a]</sup>

**Abstract:** The sequential cycloaddition of nitroalkenes with methyl vinyl ether was investigated by semiempirical (PM3) and density functional methods (B3LYP/6-31G\*). The asymmetric version was also examined with a *threo*-configured carbohydrate auxiliary. This produces a larger, more flexible system that complicates the calculation. Most transition structures were then fully optimized at the PM3 level and further refinement was done at ab initio levels. This study represents a model case that enables the rationalization of the high

facial selectivity observed in carbohydrate-based nitron- and nitronate-alkene cycloadditions. The selective *endo* orientation of the [4+2] pathway results from Coulombic attraction and secondary orbital interactions in the transition state. The stereochemical outcome is largely influenced by a combination of steric shielding from the bulky chiral

substituent at C4 and the anomeric effect that places the nitronate C6-alkoxy group in a pseudoaxial arrangement. The resulting conformation favors the subsequent *exo* approach of methyl vinyl ether to the less hindered *re* face of the nitronate. It is also remarkable to note that solvation energies stabilize significantly a particular transition structure, thereby explaining the marked stereoselection observed in a polar medium.

**Keywords:** carbohydrates • cycloadditions • domino reactions • solvent effects • theoretical calculations

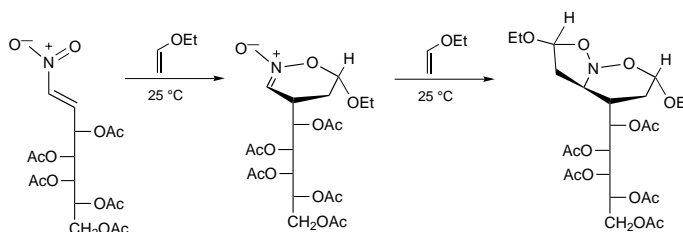
## Introduction

Numerous syntheses of naturally occurring substances and complex skeletons use a series of reactions in sequence to arrive at an overall transformation. These elegant processes called domino or tandem reactions constitute a powerful methodology in the laboratory.<sup>[1]</sup> However, the combination of simple steps to effect a complex change in the substrate may result in a continuous decrease in the stereoselectivity. As in the case of many other reactions employed in synthesis, interest in the use of carbohydrate substrates as a means to obtain optically active organic targets has been fine-tuned most impressively and has a longstanding tradition.<sup>[2]</sup> It is not, therefore, surprising that carbohydrates were examined as substrates, either as stereodifferentiators or auxiliaries, for cycloadditions that provide rapid access to a variety of ring systems.<sup>[3]</sup> Our research group has been involved in different heterodiene and heterodienophile systems, with a recent focus on sugar nitroalkenes that serve as the diastereodifferentiators.<sup>[4]</sup> Sequential reactions based on nitroalkenes have been

employed in the stereocontrolled construction of amino alcohols,<sup>[5]</sup> isoxazolines,<sup>[4, 5]</sup> elongated carbohydrates,<sup>[4]</sup> or alkaloid nuclei<sup>[6]</sup> after selective cleavage of a highly functionalized polycyclic system.

In our initial work, we observed that a carbohydrate heterodiene bearing an acyclic chain of *D-galacto* configuration reacted with ethyl vinyl ether (EVE) in a sequence of two mild reactions: the first involves a [4+2]-Diels–Alder cycloaddition followed by a second 1,3-dipolar cycloaddition between the resulting nitronate and EVE (Scheme 1).<sup>[4a]</sup> These two processes could be condensed into a one-pot three-component coupling reaction, which, if we start from the nitroalkene, EVE, and an electron-deficient alkene, gives rise to a complex cyclic structure by a domino reaction.<sup>[4c,d]</sup> In contrast to what we had expected, the effect of ethanol as

[a] Prof. Dr. P. Cintas, Prof. Dr. M. Avalos, Prof. Dr. R. Babiano, Prof. Dr. J. L. Jiménez, Prof. Dr. J. C. Palacios, Dr. M. A. Silva, J. L. Bravo  
Departamento de Química Orgánica, Facultad de Ciencias  
Universidad de Extremadura, E-06071 Badajoz (Spain)  
Fax: + (34) 924-271-149  
E-mail: pecintas@unex.es



Scheme 1. Diastereoselective carbohydrate-based domino [4+2]/[3+2] cycloaddition.

solvent was critical to achieve both high yield and high selectivity.

The problem of diastereofacial preference of carbohydrate-based cycloadditions is a current challenge.<sup>[3, 7]</sup> The most predictable face selectivity has been observed in cyclic partners in which the facial-differentiating elements are relatively fixed in the carbon or heteroatom framework, whereas less predictability is encountered in acyclic sugars for which the accurate geometry of the transition structure (TS) for the cycloaddition can only be determined by computation. Therefore, we have undertaken the study of the molecular mechanism for this relevant domino reaction. The results give us an insight into the concept of diastereodifferentiation in the acyclic series and can be used to assess the predictive power of schemes grounded in molecular orbital (MO) theory.

## Computational Methods

All gas-phase calculations were carried out with the Gaussian 94 package of programs.<sup>[8]</sup> A detailed characterization of the potential energy surface was carried out at the PM3 level<sup>[9]</sup> to ensure that all stationary points were located and properly characterized, and with complete optimization of bond lengths, bond angles, and dihedral angles. The stationary points were characterized by frequency calculations in order to verify that the TSs have one and only one imaginary frequency. Likewise, the PM3 geometries were used as a starting point in the search of the B3LYP/6-31G\* structures, by means of *ab initio*<sup>[10]</sup> and DFT calculations that use the B3LYP hybrid functional.<sup>[11]</sup>

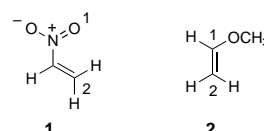
The solvent effects were considered by B3LYP/6-31G\* single-point calculations by using a self-consistent reaction field (SCRF)<sup>[12]</sup> method, based on the Onsager model,<sup>[13]</sup> in which the solvation energy was

**Abstract in Spanish:** *Se han investigado las cicloadiciones secuenciales de nitroalquenos con metil vinil éter mediante cálculos semiempíricos (PM3) y funcionales de densidad (B3LYP/6-31G\*). Se ha considerado también la versión asimétrica de este proceso con un fragmento de carbohidrato de configuración treó. Esto complica el cálculo debido al incremento del tamaño molecular y la flexibilidad conformacional inducida por este grupo. Por ello, la mayoría de las estructuras de transición fueron optimizadas a nivel PM3 y luego refinadas a nivel ab initio. Este estudio permite racionalizar la alta selectividad facial observada en numerosas cicloadiciones de nitronas y nitronatos a alquenos usando auxiliares quirales derivados de carbohidratos. La orientación selectiva endo de la etapa [4+2] resulta de atracción Coulombica e interacciones orbitales secundarias en el estado de transición. El curso estereoquímico está influenciado en gran medida por una combinación del apantallamiento estérico producido por el voluminoso sustituyente quiral en la posición C4, y el efecto anómero que sitúa al grupo alcoxi de la posición C6 del nitronato con una orientación pseudoaxial. La conformación resultante favorece el posterior ataque exo del metil vinil éter por la cara re menos impedida del nitronato. Conviene señalar que las energías de solvatación contribuyen a estabilizar una determinada estructura de transición, explicando de esta forma la observación experimental de una elevada estereoselectividad en un disolvente polar.*

calculated from the electrostatic energy between the solute, modeled as a dielectric sphere of radius  $a_0$ , and the solvent, ethanol in the present study, described as a continuum of dielectric constant  $\epsilon = 24.3$ .

## Results and Discussion

**Regiochemistry:** Theoretical calculations of the energies of the frontier orbitals and TSs were performed at a semiempirical level, which we were constrained to employ because of the complexity of the system under study (Scheme 1). Model compounds **1** and **2** reproduce the structural characteristics of the partners in this archetypal domino cycloaddition.



The frontier-orbital calculations (FMO)<sup>[14]</sup> predict the tendency of substrates to react in an inverse LUMO<sub>diene</sub>-controlled Diels–Alder reaction because the energy gap HOMO<sub>dienophile</sub>–LUMO<sub>diene</sub> ( $\Delta E = 8.65$  eV) is lower than the energy of the interaction HOMO<sub>diene</sub>–LUMO<sub>dienophile</sub> ( $\Delta E = 13.28$  eV). Table 1 depicts energies and the coefficients ( $c_1$  and  $c_2$ ) of the frontier orbitals, either at PM3 or *ab initio* levels, which justify the regiochemistry of the [4+2]-cycloaddition

Table 1. HOMO/LUMO energies [eV] and coefficients calculated by semiempirical and *ab initio* methods for compounds **1** and **2**.

	MO	PM3	$c_1$	$c_2$	HF/6-31G*	$c_1$	$c_2$
<b>1</b>	HOMO	-12.03	0.73	-0.44	-11.84	0.15	-0.35
	LUMO	-0.97	0.30	0.74	1.80	0.24	0.27
<b>2</b>	HOMO	-9.62	0.45	0.65	-9.06	0.30	0.38
	LUMO	1.25	0.81	-0.75	5.50	0.38	-0.31

step observed in the experimental work. Likewise, there is a secondary orbital interaction between the nitrogen atom on the nitroalkene and the vinyl ether oxygen, thereby accounting for an *endo* orientation (Figure 1).

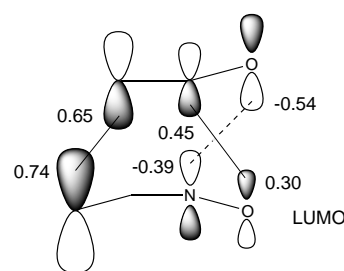
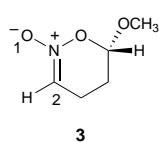


Figure 1. Secondary orbital interaction observed for the *endo* orientation of the [4+2] cycloaddition.

With regard to the regiochemistry of the [3+2] cycloaddition, model compounds **2** and **3** have been equally utilized. Table 2 collects the energies and coefficients of their frontier orbitals at PM3 level. Again, an inspection of the two possible energy gaps reveal that the reactivity is controlled by



LUMO<sub>dipole</sub>–HOMO<sub>dipolarophile</sub> interaction; this is in agreement with a type-III 1,3-dipolar cycloaddition.<sup>[15]</sup>

Such an interaction is enough to force the reaction into the observed orientation.

Table 2. HOMO/LUMO energies [eV] and coefficients estimated by PM3 calculations for compounds **2** and **3**.

	MO	PM3	c <sub>1</sub>	c <sub>2</sub>
<b>2</b>	HOMO	–9.62	0.45	0.65
	LUMO	1.25	0.81	–0.75
<b>3</b>	HOMO	–9.58	0.49	–0.60
	LUMO	0.41	0.36	0.52

Nevertheless, the opposite interaction of the nitronate HOMO with the vinyl ether LUMO cannot be underestimated, because the difference between these interactions is small ( $\Delta E = 0.8$  eV). The difficulty with this approach, however, can be solved taking into account the existence of a secondary bonding interaction between frontier orbitals that lowers the energy of the *endo* reaction path (Figure 2). This contrasts with the fact that the *exo* adduct is experimentally observed,<sup>[4a]</sup> presumably for steric reasons.

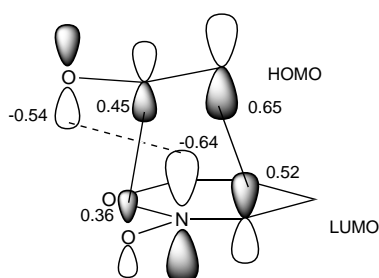
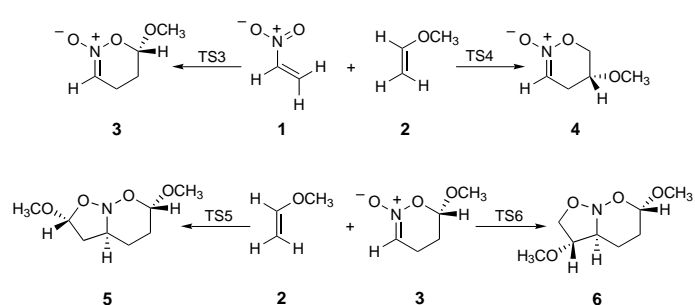


Figure 2. Secondary orbital interactions for the *endo* reaction path of the [3+2] cycloaddition.

To clarify this question we carried out a thermodynamic and kinetic study of the domino process. The imaginary frequencies and corresponding geometries were obtained for the TSs of the four cycloadditions depicted in Scheme 2. Schematic representations of the energy profiles for [4+2] and [3+2] cycloadditions (Figure 3) evidence that the *exo* regioisomer **5** is both kinetically and thermodynamically the more stable. These cycloadditions are exothermic processes characterized by early transition structures.

**The [4+2] cycloaddition—stereochemistry:** From the kinetic and thermodynamic analysis, we could easily justify that the cycloaddition proceeds regioselectively to give only one bicyclic fused system. Next, the stereochemical result of experiment was investigated by using the model reaction outlined in Scheme 3.<sup>[16]</sup> The absence of stereogenic centers in



Scheme 2. Models studied for Diels–Alder and 1,3-dipolar cycloadditions.

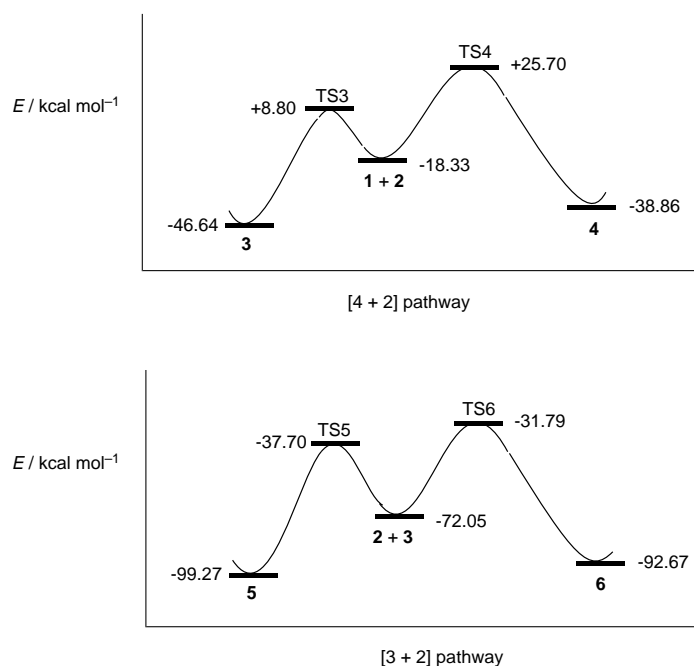
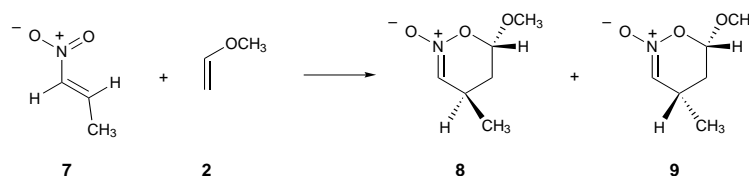


Figure 3. Energy level diagrams of [4+2] and [3+2] cycloadditions studied in this work.



Scheme 3. Possible nitronates resulting from [4+2] cycloaddition of an achiral  $\beta$ -substituted nitroalkene and methyl vinyl ether.

the starting heterodiene **7** would lead to two different stereoisomers (**8** and **9**), which would be able to adopt two possible conformations (**8a,b/9a,b**).

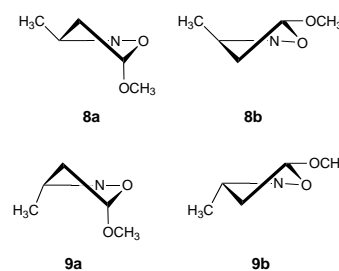


Table 3 shows the enthalpies of formation for both conformers along with the potential-energy barriers associated with **TS8** and **TS9**, and the lengths of the O1–C6 and C4–C5 bonds formed in the [4+2] step. Data from Table 3 evidence the greater stability of conformers **8a** and **9a**, a fact attributable to the anomeric effect.<sup>[17]</sup> It is the anomeric

Table 3. Heats of formation [kcal mol<sup>-1</sup>] and lengths of forming bonds [Å] for cycloadducts and transition structures **8** and **9**.

	Cycloadducts				Transition structures	
	<b>8a</b>	<b>8b</b>	<b>9a</b>	<b>9b</b>	<b>TS8</b>	<b>TS9</b>
$\Delta H_f$	-52.12	-49.61	-51.07	-49.87	2.14	2.66
O1–C6	1.398	1.415	1.389	1.414	2.608	2.648
C4–C5	1.527	1.526	1.526	1.526	1.762	1.780

substituent (OMe), which occupies an axial orientation, that exerts the larger directing effect in the Diels–Alder reaction. In both cases, the 1,2-oxazine ring adopts a half-chair conformation in which the anomeric carbon C6 is below the plane of O1–N2–C3–C4.

The lengths of the C4–C5 bonds in **TS8** and **TS9** are 1.762 and 1.780 Å, respectively, whereas the distances between O1–C6 are 2.608 and 2.648 Å, respectively. The optimized geometries for cycloadducts and TSs (Figure 4) suggest a concerted process with a large degree of asynchronicity. Consequently, there is more bond formation at the  $\beta$ -carbons (they are more nucleophilic) in the transition structures; this is reminiscent of a Michael type addition.

The *endo* preference may be explained in terms of a stabilizing electrostatic interaction between the electron-rich

oxygen on the enol ether and the charged nitrogen atom on the heterodiene. This favorable interaction cannot be reached in an alternative *exo* orientation. Boger has also explained the *endo* orientation on the basis of a similar hyperconjugative anomeric-type interaction in which the lone pair of electrons on the diene or a dipole oxygen ( $n_O$ ) interact with the  $\sigma^*_{CO}$  orbital of the ether, therefore stabilizing the *endo* TS when arranged in an antiperiplanar arrangement.<sup>[18]</sup> The **TS9** is less stable ( $\Delta E = 0.52$  kcal mol<sup>-1</sup>) because the stabilizing Coulombic interaction does not compensate the steric hindrance of such substituents that become closer.

A salient feature that concerns the conformation of methyl vinyl ether is the switch during the course of reaction from *s-cis* in the reactant to *s-trans* in the transition structure. This contrasts with the ground-state *s-cis* conformation of methyl vinyl ether, which is favored by 1.66 kcal mol<sup>-1</sup>. This conformational switching has been recently analyzed by Houk et al. by theoretical calculations and experimental tests.<sup>[19]</sup> Accordingly, the preferred conformation can be evaluated by computation, but there is no direct way to detect which conformation is present in the TS of the reaction. Houk et al. hypothesized that enol ethers fixed in different conformations will react at different rates, and they were able to test this prediction for the cycloadditions of several enol ethers with conjugated nitroso compounds and nitrones.<sup>[19]</sup>

To verify experimentally the latter point in the present study, we attempted a series of cycloadditions with a chiral nitroalkenyl sugar. No reaction was observed with 2,3-dihydrofuran after several days at room temperature. Then, we turned our attention towards a competitive process that involves the chiral nitroalkene and ethyl vinyl ether plus 2,3-

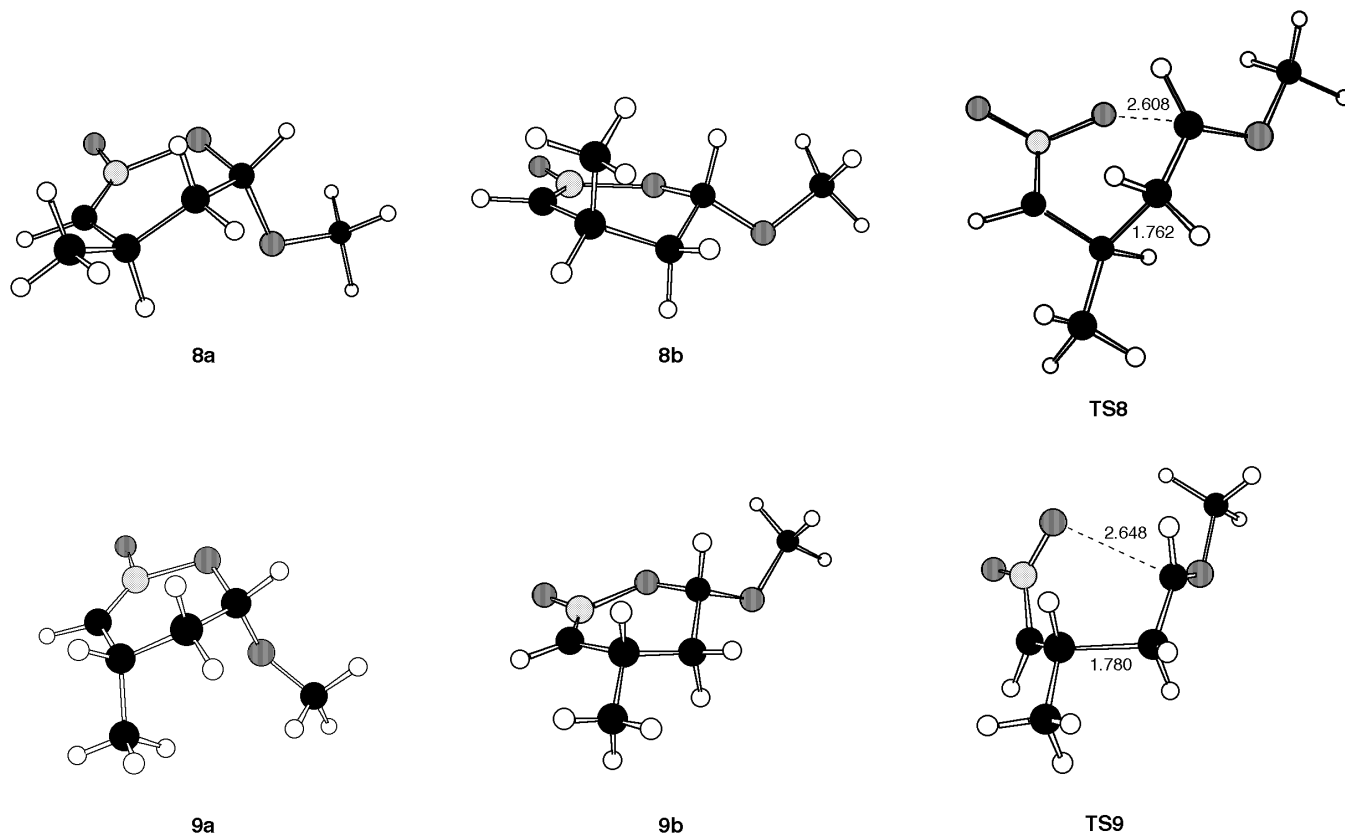
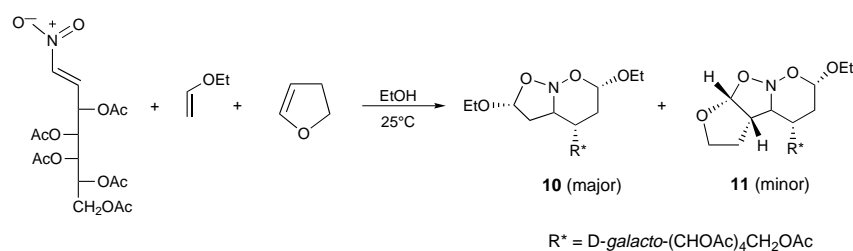


Figure 4. Cycloadducts and transition structures obtained by reaction of nitroalkene **7** and methyl vinyl ether.



Scheme 4. Competitive domino cycloaddition of a chiral nitroalkene in the presence of ethyl vinyl ether and 2,3-dihydrofuran.

dihydrofuran under the reaction conditions reported previously (Scheme 4).<sup>[4a]</sup>

As expected, the domino process took place preferentially with EVE to yield **10** as the major adduct and as a single stereoisomer. A minor product (**11**) could also be separated by crystallization in 10% yield. Although this crystalline material was not suitable for an X-ray crystallography study, from proton and carbon NMR experiments we could easily establish that the cycloaddition also proceeded stereospecifically with 2,3-dihydrofuran and the formation of the domino adduct **11**.<sup>[20]</sup> The structure was determined from the coupling constants in the <sup>1</sup>H NMR spectrum. The value of  $J_{9a,3a} = 5.3$  Hz is identical to that observed for analogous protons in adduct **10**, thereby evidencing the same stereochemical outcome. The presence of a triplet at highfield ( $\delta = 1.26$ ) is consistent with the incorporation of only one EVE moiety. Furthermore, the appearance of two additional carbon resonances at  $\delta = 67.3$  and  $27.3$ , attributable to methylene groups (DEPT experiment), suggests the assembly of a tetrahydrofuran skeleton. The product ratios of these cycloadditions reflect an exclusive reactivity of EVE for the Diels–Alder reaction and a preferential one for the 1,3-dipolar cycloaddition.

Although Houk et al. have shown that, in the case of enol ethers, a polar solvent can stabilize the *s-cis* TS more relative to the *s-trans* TS,<sup>[19]</sup> the acyclic enol ether can adopt the *s-trans* conformation anyway in the cycloaddition transition state. Conversely, the conformationally fixed 2,3-dihydrofuran constrained to be *s-cis* accounts for its inertness towards the domino process.

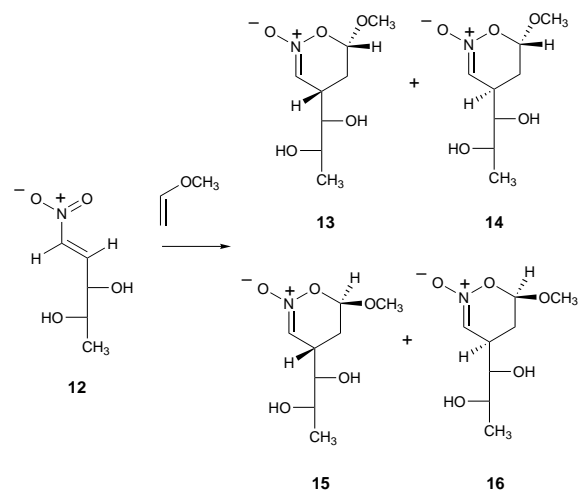
**The [4+2] cycloaddition—influence of the carbohydrate chain:** So far, the absence of chirality in the heterodiene impedes a rationale for the facial selectivity. We have therefore incorporated an *L-threo*-configured side chain into the heterodiene to account for the observed stereoselection (Scheme 5).

Again, the computational study was done at the PM3 level, owing to the increased size of reactants and adducts, and the presence of several heavy atoms. Adducts **13–16** arise from *endo* and *exo* approaches, for which the enol ether can also access the *re* and *si* faces of the heterodiene (Scheme 6, Table 4).

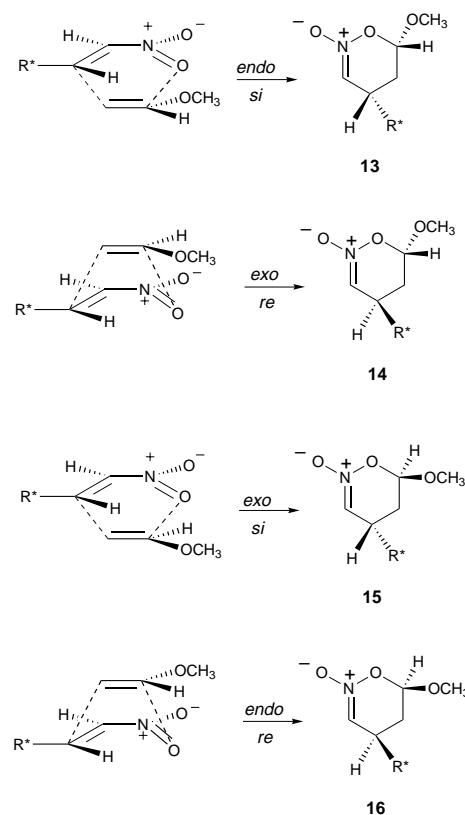
Figure 5 displays the optimized transition structures **TS13–TS16**. The bulky chiral substituent at C4 adopts a pseudo-equatorial arrangement, a fact that may be partly responsible for the twist-boat conformation of the six-membered ring. On

the other hand, it is likely that the alkoxy group at C6 prefers the axial position because of a stabilizing anomeric effect,<sup>[17]</sup> thereby accounting for the greater stability of adducts **13**, **15**, and **16**.

Figure 5 also reveals the asynchronicity of the cycloadditive process with a pronounced Michael type addition



Scheme 5. Chiral nitronates generated by Diels–Alder cycloaddition of nitroalkene **12** and methyl vinyl ether.



Scheme 6. Stereoselection and facial selectivity issues for [4+2] cycloadditions.

Table 4. Enthalpies of formation [kcal mol<sup>-1</sup>] and lengths of forming bonds [Å] for cycloadducts and transition structures **13**–**16**.

	Cycloadducts				Transition structures			
	<b>13</b>	<b>14</b>	<b>15</b>	<b>16</b>	<b>TS13</b>	<b>TS14</b>	<b>TS15</b>	<b>TS16</b>
$\Delta H_f^\ddagger$	-142.19	-138.26	-143.25	-142.01	-89.25	-85.32	-89.51	-88.13
O1–C6	1.398	1.415	1.397	1.397	2.789	2.786	2.710	2.640
C4–C5	1.529	1.525	1.527	1.529	1.799	1.812	1.785	1.797
$\mu$	1.47	2.24	1.52	1.32	2.92	2.41	2.93	2.83

character. As illustrated in TSs the long distance between the nitrogen atom and the methoxy group of the incoming dienophile is such that the stabilizing effects that may be present (secondary orbital interactions, Coulombic attraction, and the incipient anomeric effect developed in the TS) are eliminated. The enhanced stability of **TS13** and **TS15** results from steric effects, since the chiral carbohydrate effectively protects one diastereoface of the heterodiene unit. In both cases, the *re* face is blocked and the enol ether approaches from the more accessible *si* face.

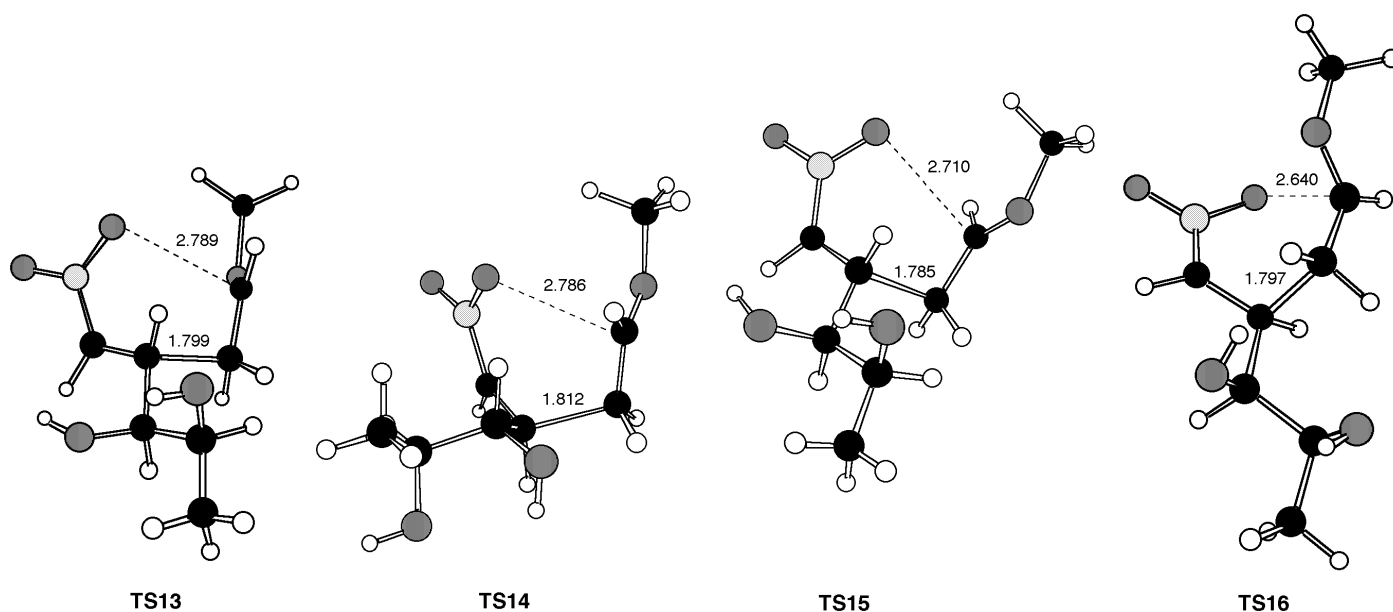
A further B3LYP/6-31G\* calculation on the **TS13** and **TS15** evidences an inversion in stabilities when compared with the results at the PM3 level, because **TS13** is slightly more stable, by 0.16 kcal mol<sup>-1</sup>, than **TS15**. This suggests that a refined method is able to provide a better explanation of the selectivity found experimentally.

Even though the preferential approach may be due to electrostatic and steric effects, the solvation of TSs cannot be neglected. Unlike Diels–Alder reactions that have relatively nonpolar TSs,<sup>[21]</sup> those of the hetero-Diels–Alder cycloadditions may have significant polarity. Table 4 also lists the gas-phase dipole moments of the cycloadducts and TSs. Although there is no difference between the polarity of **TS13** and **TS15** (2.92 D versus 2.93 D), a polar solvent could likely change the relative energies of these structures. A B3LYP/6-31G\* calculation was used on the SCRF model to determine the relative energies of each TS placed in a solvent cavity of dielectric constant 24.3 of ethanol,<sup>[22]</sup> which is used experimentally for the domino process.

The **TS13** is 1.08 kcal mol<sup>-1</sup> lower in energy than **TS15** in an SCRF cavity of ethanol. Moreover, the difference between the dipole moments of the TSs increases in this medium ( $\mu = 3.08$  D for **TS13** and 2.94 D for **TS15**). Thus, when we consider the change in the energy difference produced by the solvent, then the Onsager B3LYP model is in the closest agreement with the structure of the nitronate obtained in the experiment (Scheme 1, *vide supra*). Ethanol is a rather uncommon solvent in Diels–Alder reactions. Since striking selectivities have been observed for such cycloadditions in polar solvents,<sup>[23]</sup> it is not surprising that solvation energies stabilize significantly a particular TS.

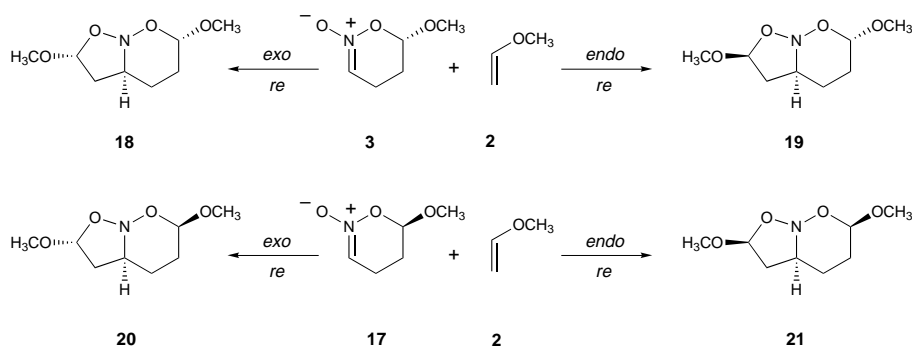
**The [3+2] cycloaddition route:** The dipolar cycloaddition of the first-formed nitronate largely dictates the stereochemical outcome in view of the stereoelectronic characteristics imposed by this intermediate. In general, intermolecular [3+2] cycloadditions proceed with varying degrees of stereocontrol (*endo* versus *exo* approach) and facial selectivity.<sup>[24]</sup> In a recent study, Denmark et al. analyzed the stereochemical course of [3+2] cycloadditions of cyclic nitronates with a series of mono- and disubstituted dipolarophiles.<sup>[25]</sup> They carried out theoretical studies at the RHF and B3LYP levels for predicting regioselectivity and found that an *exo* selection is generally favored owing to steric effects.

Since preparative chemistry evidences that the cycloadditions of chiral nitronates bearing a *L-threo* side chain are highly facially selective,<sup>[4a,c,d]</sup> a systematic study of this dipolar process was undertaken. At first, two sources of facial bias

Figure 5. Chairlike transition structures **13**–**16**.

should be evaluated: the anomeric effect and, as before, the influence provided by a neighboring chiral inductor. To better understand the role of an alkoxy group at C6, nitronates **3** and **17**, which bear an enantiomeric relationship, were chosen as simplified models for the [3+2] cycloaddition with methyl vinyl ether (Scheme 7). Geometries for cycloadducts **18–21** were fully optimized at the PM3 level and Table 5 lists their energies, dipole moments, and lengths of the forming bonds.

In all cases, we considered that the dipolarophile approached the *re* face of each of the nitronates **3** and **17** exclusively;



Scheme 7. Dipolarophile approach to nitronates **3** and **17**.

Table 5. Enthalpies of formation [kcal mol<sup>-1</sup>], lengths of forming bonds [Å], and dipole moments [Debyes] for cycloadducts **18–21**.

	<b>18</b>	<b>19</b>	<b>20</b>	<b>21</b>
$\Delta H_f$	-99.27	-98.82	-98.44	-97.84
O1–C2	1.422	1.411	1.421	1.422
C3–C3a	1.529	1.533	1.530	1.533
$\mu$	1.97	1.43	1.41	0.75

this halves the number of possible cycloadducts, since the alternative *exo* and *endo* approaches to the *si* face are equally possible and would lead to their enantiomeric partners. Enantiomeric pairs result from the fact that *cis*-fused rings exhibited greatly enhanced stability ( $\Delta E_{cis/trans} = 6.6–10.8$  kcal mol<sup>-1</sup>) and from the easy configurational inversion on endocyclic nitrogen. Although the most stable cycloadduct (**18**) has the same configuration as the diastereomer observed experimentally, the energy differences are small and would be consistent with a poor stereoselectivity.

If the stereochemical outcome were due to an anomeric effect, the conformation of the six-membered nitronate and the conformations of the two methoxy groups would affect the stability of the TSs leading to adducts **18–21**. Although the 1,2-oxazine ring adopts a boat-like conformation in the ground state, this ring may fold into a chair as the reaction progresses from transition state to product.

In their study on nitronates, Denmark et al. found that a

chairlike conformation facilitates a nearly antiperiplanar arrangement of the nitrogen lone-pair and the C–O bond.<sup>[25]</sup> Accordingly, the key stereochemical issues are ring conformation (chairlike or boatlike) and conformation of methoxy group around the C–O bond (*s-cis* or *s-trans*). Overall this gives, in the case of **18**, a set of eight possible TSs from nitronate **3** (Figure 6).

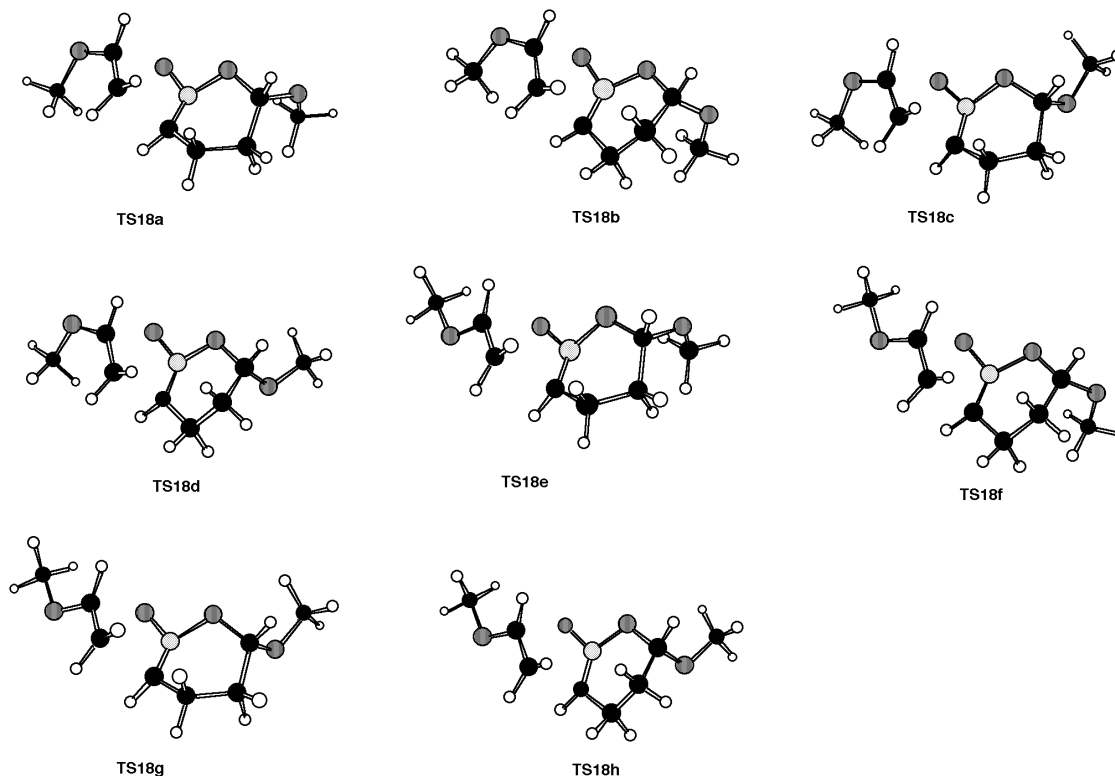


Figure 6. Chairlike and boatlike transition structures of nitroso acetal **18**.

Table 6 shows the calculated energies for TSs taking into account such a conformation analysis. From these data, it is clear that in the transition state the chairlike conformation is preferred for the six-membered ring and the C6–OMe bond

Table 6. Conformation analysis and energies [calmol<sup>-1</sup>] for transition structures **18a–h**.

	C2-OMe conformation	C6-OMe conformation	1,2-oxazine conformation	$\Delta H_f$
<b>TS18a</b>	<i>cis</i>	<i>cis</i>	boatlike	–34.28
<b>TS18b</b>	<i>cis</i>	<i>cis</i>	chairlike	–35.37
<b>TS18c</b>	<i>cis</i>	<i>trans</i>	boatlike	–35.25
<b>TS18d</b>	<i>cis</i>	<i>trans</i>	chairlike	–37.54
<b>TS18e</b>	<i>trans</i>	<i>cis</i>	boatlike	–34.65
<b>TS18f</b>	<i>trans</i>	<i>cis</i>	chairlike	–35.66
<b>TS18g</b>	<i>trans</i>	<i>trans</i>	boatlike	–35.43
<b>TS18h</b>	<i>trans</i>	<i>trans</i>	chairlike	–37.70

adopts a *s-trans* conformation. Nevertheless, the conformation of the C2–OMe bond has little or no influence. Once these favorable conformational patterns were fixed, the energies for the TSs leading to **19–21** were equally calculated. Again, the effect of the vinyl ether conformation on the stability of TSs was minimal (Table 7).

A simple inspection of the energies listed in Tables 6 and 7 enables us to predict that adducts **18** and **19** would be prevalent. There are no significant effects to stabilize either transition state ( $\Delta E = 0.38$  kcalmol<sup>-1</sup>). Both cycloadducts would have arisen from an approach of the vinyl ether to the *re* face of the nitronate, which is the less hindered face, and the approach of the dipolarophile to the face opposite the C6–OMe group. In nitronate **17**, such a group impedes to

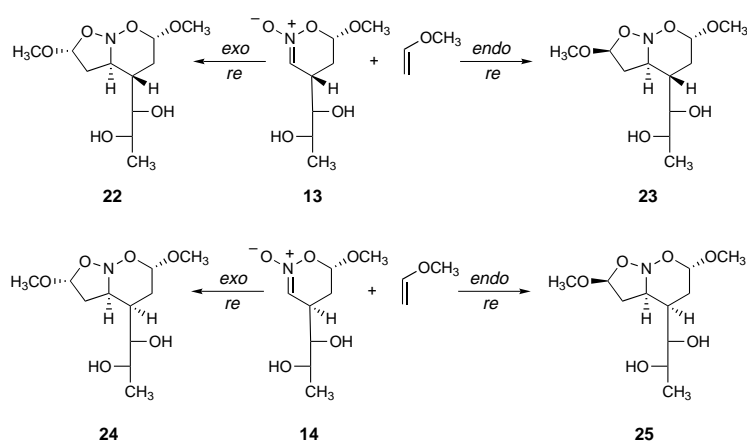
Table 7. C2-alkoxy group conformation and energies [kcalmol<sup>-1</sup>] for transition structures **19–21**.

	C2-OMe conformation	$\Delta H_f$
<b>TS19a</b>	<i>cis</i>	–36.71
<b>TS19b</b>	<i>trans</i>	–37.32
<b>TS20a</b>	<i>cis</i>	–34.77
<b>TS20b</b>	<i>trans</i>	–35.04
<b>TS21a</b>	<i>cis</i>	–34.30
<b>TS21b</b>	<i>trans</i>	–34.24

Table 8. Enthalpies of formation [kcal mol<sup>-1</sup>], lengths of forming bonds [Å], and dipole moments [Debyes] for cycloadducts and transition structures **22–25**.

	Cycloadducts				Transition structures			
	<b>22</b>	<b>23</b>	<b>24</b>	<b>25</b>	<b>TS22</b>	<b>TS23</b>	<b>TS24</b>	<b>TS25</b>
$\Delta H_f$	–195.99	–195.25	–191.63	–189.86	–132.62	–129.45	–130.08	–134.39
O1–C2	1.422	1.414	1.421	1.413	2.081	2.073	2.079	2.043
C3–C3a	1.534	1.535	1.531	1.532	2.110	2.120	2.119	2.127
$\mu$	1.89	1.45	2.11	1.52	1.56	1.69	1.33	0.55

access the enol ether from the *re* face. Since **TS18** and **TS19** only differ in orientation (*exo* versus *endo*), this result mismatches the experimentally determined high facial selectivity. As before, we sought the origin of stereoselection in the steric bulk of the carbohydrate chain at C4. Replacment of a hydrogen atom with a chiral open-chain substituent of *L-threo* configuration dramatically affects the geometries of adducts and their relative energies. The vicinal diol inhabits a pseudoequatorial position, thereby folding the six-membered ring into a chair in the transition state. Scheme 8 outlines the four possible pathways from nitronates **13** and **14**, for which the dipolarophile approaches the less sterically congested *re* face. The enthalpies of the resulting cycloadducts and their TSs (**22–25**) together with dipole moments and distances between atoms that represent the forming bonds are collected in Table 8. The chairlike TSs depicted in Figure 7 reveal a



Scheme 8. Dipolarophile approach to chiral nitronates **13** and **14**.

slight asynchronous character of the [3+2] cycloaddition as well.

Given the exothermicity of these processes, the relative stability of cycloadducts cannot be inferred from those of the early TSs. The orientation of the chiral substituent at C4 with respect to the isoxazolidine ring (*exo* for **22** and **24**, *endo* for **23** and **25**) should be responsible for the greater stability of adducts **22** and **23**.

In accord with data from Table 8, the cycloaddition would preferentially afford **25** through the most stable **TS25**. However, the latter stems from an *endo* approach to the *re* face of the chiral nitronate **14**, a fact that disagrees with the experimental observation in which a structure closely related to **22** was obtained as a single diastereomer. As suggested before for the [4+2] cycloaddition, this results allows us to establish that only one nitronate, configurationally related to



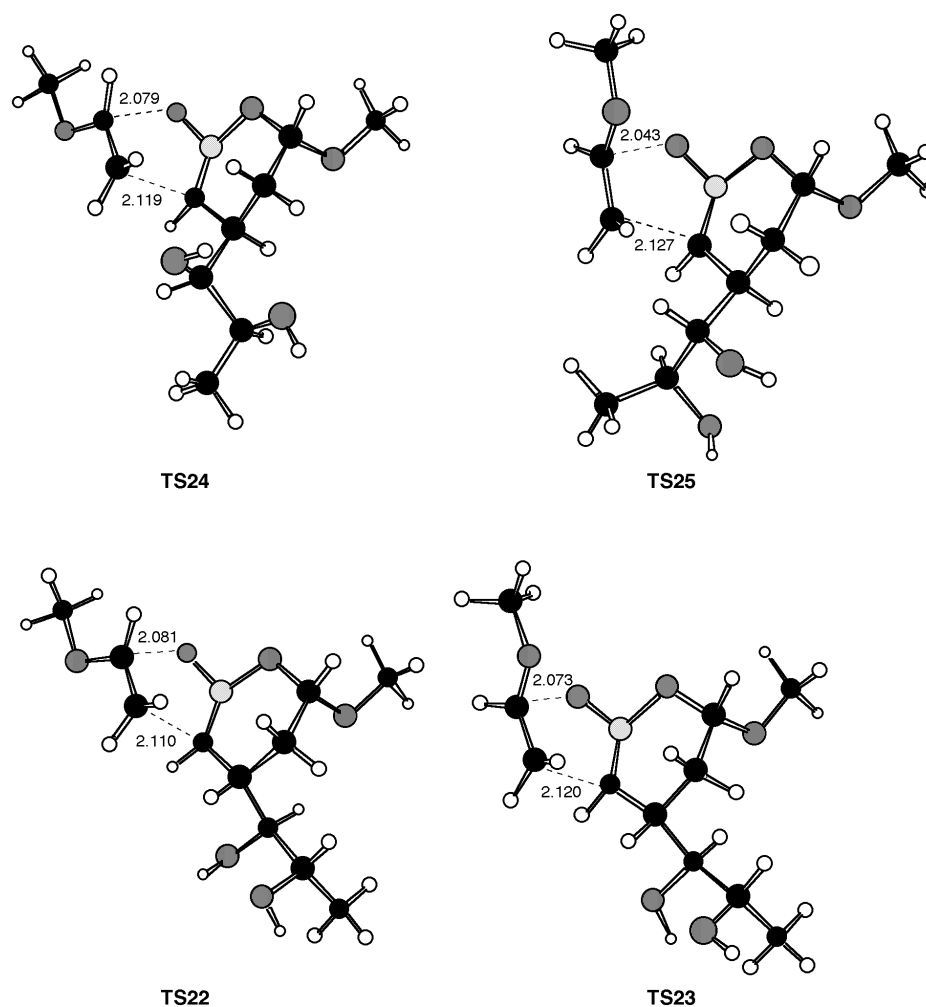


Figure 7. Transition structures 22–25.

**13**, should be formed in the first step of the domino process. That the *exo* orientation occurs selectively in the [3+2] pathway is evidenced by the enhanced stability of the **TS22** with respect to **TS23** ( $\Delta E = 3.17 \text{ kcal mol}^{-1}$ ). The B3LYP/6-31G\* calculation augments the difference still further ( $\Delta E = 5.88 \text{ kcal mol}^{-1}$ ). Since the **TS23** exhibits a higher polarity, a polar medium should be able to stabilize it more relative to the **TS22**. Solvation energies were then examined with the aid of a SCRF Onsager model at the B3LYP/6-31G\* level. Even under such circumstances the **TS22** is  $5.50 \text{ kcal mol}^{-1}$  lower in energy. Again, these results do justify the consideration of solvent effects to reach values that are in pretty good agreement with the experimental data.

In the present study the facial selectivity is largely due to steric effects from the chiral nitroalkene auxiliary. One would expect that these would be mitigated by both the longer distance between the reaction center and the first stereogenic centers of the side chain (which feature a relative *threo* arrangement in a *D-galacto* configuration), and the flexibility of the acyclic carbohydrate moiety. However, a consideration of the energies of the competing transition structures permit a greater steric discrimination. Likewise, if because of an inherent asymmetric environment one side of the  $\pi$  orbital extends further into space than the other, it will overlap better

with the approaching dienophile and, therefore, afford the forming bonds a greater degree of stabilization.

It has been demonstrated that nitrones which carry a chiral auxiliary derived from carbohydrates may display high levels of diastereoselectivity in [3+2] cycloadditions.<sup>[26]</sup> The work by Saito and co-workers, who described [3+2] cycloadditions of nitrones to a chiral allylic ether with a high diastereofacial differentiation, is especially relevant.<sup>[27]</sup> This last compound, accessible from *L*-tartaric acid, bears a vicinal diol controller with a relative *threo* configuration that discriminates  $\pi$  faces of dipolarophile. A high stereodifferentiation of the  $\pi$  faces of the nitron has also been achieved by the same authors, but with incorporation of the diol in the nitron component.<sup>[28]</sup> This type of uncatalyzed process is especially notable, because the use of 1,3-dipoles is often incompatible with Lewis acid catalysts. Likewise, a recent work describes high levels of acyclic stereodifferentiation in intramolecular nitron-alkene cycloadditions of 3-*O*-allylmonosaccharides with *threo* configuration at the adjacent chiral tether.<sup>[29]</sup>

**Cycloaddition versus glycosidation:** Anyone familiar with carbohydrate chemistry will recognize that the above-mentioned sugar-based nitroso acetals are in fact homologated *O*-glycosides.<sup>[30]</sup> Consequently, in spite of the theoretical inter-

pretation provided in this work, it is still unclear if the stereocontrolled formation of nitroso acetals arises from a cycloaddition pathway or a stereospecific *O*-glycosidation involving ethanol as the glycosyl acceptor molecule. In the latter case, a hydroxyl-containing compound could be incorporated as the aglycone at the pseudoglycosidic centers of the five- and six-membered rings. The mechanism would involve the formation of a hemiacetal intermediate followed by the attack of a lower alcohol to afford the nitroso acetal again. To rule out this alternative pathway, the synthetic process outlined in Scheme 1 was performed with excess of EVE, but with *methanol* as solvent.<sup>[31]</sup> A careful analysis of the reaction mixture revealed the exclusive formation of a nitroso acetal, which was identical to product obtained in ethanol.<sup>[4a]</sup> No MeO-containing compounds could be detected at all. This agrees with a cycloadditive process in which a carbohydrate auxiliary strongly influence the steric course.

## Conclusions

In this paper a theoretical interpretation of asymmetric domino Diels–Alder/1,3-dipolar cycloadditions of nitroalkenes and vinyl ethers has been reported. The stereodifferentiating element was introduced on the heterodiene as a carbohydrate-based tether with *threo* configuration. This study also serves as a model case to explain the high stereoselectivity in the cycloadditions of nitroalkenyl sugars with olefins that involves the intermediacy of nitrones and nitronates. From a mechanistic viewpoint, the domino process consists of two concerted and asynchronous cycloadditions. Theoretical calculations support the existence of Michael type transition structures. Also of note is the *s-trans* preference of enol ethers in transition structures, a fact that has also been verified with a conformationally fixed enol ether. The *endo* approach of methyl vinyl ether to the heterodiene is a consequence of secondary orbital interactions that produce a transition structure wherein the six-membered ring adopts a half-chair conformation. The bulky substituent at C4 adopts a pseudoequatorial arrangement, whereas a stabilizing anomeric effect places the alkoxy group at C6 in a pseudoaxial orientation. The [3+2] cycloaddition takes place with an *exo* approach to the less hindered *re* face of the chiral nitronate. Interestingly, the consideration of solvation energies does justify the remarkable stereoselection observed in the experiment.

## Acknowledgments

Financial support by grants from the Ministry of Education and Culture (DGICYT, PB95-0259) and the Junta de Extremadura-Fondo Social Europeo (IPR98-C040) is gratefully acknowledged.

- [1] For reviews on domino or tandem reactions: a) T.-L. Ho, *Tandem Organic Reactions*, Wiley, New York, **1992**; b) L. F. Tietze, U. Beifuss, *Angew. Chem.* **1993**, *105*, 137–169; *Angew. Chem. Int. Ed. Engl.* **1993**, *32*, 131–163; c) R. A. Bunce, *Tetrahedron* **1995**, *51*, 13103–13159; d) L. F. Tietze, *Chem. Rev.* **1996**, *96*, 115–136; e) “Cascade Reactions”

- (Ed.: R. Grigg), *Tetrahedron, Symposia-in-Print* **1996**, *52*, 11385–11664; f) L. F. Tietze, G. Ketschau, *Top. Curr. Chem.* **1997**, *189*, 1–120; g) It should be pointed out that, in most cases, the word domino should be used since all reactions are time-resolved (one after another): see refs. [1b] and [1d].
- [2] a) H. Kunz, K. Rück, *Angew. Chem.* **1993**, *105*, 355–377; *Angew. Chem. Int. Ed. Engl.* **1993**, *32*, 336–358; b) M. Bols, *Carbohydrate Building Blocks*, Wiley, New York, **1996**; c) P. G. Hultin, M. A. Earle, M. Sudharshan, *Tetrahedron* **1997**, *53*, 14823–14870; d) H. Kunz, K. Rück-Braun, *Chiral Auxiliaries in Cycloadditions*, Wiley-VCH, Weinheim, **1998**.
- [3] *Cycloaddition Reactions in Carbohydrate Chemistry*, (Ed.: R. M. Giuliano), American Chemical Society, Washington, DC, **1992**.
- [4] a) M. Avalos, R. Babiano, P. Cintas, F. J. Higes, J. L. Jiménez, J. C. Palacios, M. A. Silva, *J. Org. Chem.* **1996**, *61*, 1880–1882; b) M. Avalos, R. Babiano, A. Cabanillas, P. Cintas, F. J. Higes, J. L. Jiménez, J. C. Palacios, *J. Org. Chem.* **1996**, *61*, 3738–3748; c) M. Avalos, R. Babiano, P. Cintas, J. L. Jiménez, J. C. Palacios, M. A. Silva, *Chem. Commun.* **1998**, 459–460; d) M. Avalos, R. Babiano, P. Cintas, F. J. Higes, J. L. Jiménez, J. C. Palacios, M. A. Silva, *J. Org. Chem.* **1999**, *64*, 1494–1502.
- [5] a) E. Marotta, P. Righi, G. Rosini, *Tetrahedron Lett.* **1998**, *39*, 1041–1044; b) P. Righi, E. Marotta, G. Rosini, *Chem. Eur. J.* **1998**, *4*, 2501–2512.
- [6] S. E. Denmark, A. Thorarensen, *Chem. Rev.* **1996**, *96*, 137–165.
- [7] a) R. W. Franck, in *Cycloaddition Reactions in Carbohydrate Chemistry*, (Ed.: R. M. Giuliano), American Chemical Society, Washington, DC, **1992**, pp. 24–32; b) R. M. Giuliano, A. D. Jordan, Jr., A. D. Gauthier, K. Hoogsteen, *J. Org. Chem.* **1993**, *58*, 4979–4988.
- [8] a) M. J. Frisch, G. W. Trucks, H. B. Schlegel, P. M. W. Gill, B. G. Johnson, M. A. Robb, J. R. Cheeseman, T. Keith, G. A. Petersson, J. A. Montgomery, K. Raghavachari, M. A. Al-Laham, V. G. Zakrzewski, J. V. Ortiz, J. B. Foresman, J. Cioslowski, B. B. Stefanov, A. Nanayakkara, M. Challacombe, C. Y. Peng, P. Y. Ayala, W. Chen, M. M. Wong, J. L. Andres, E. S. Replogle, R. Gomperts, R. L. Martin, D. J. Fox, J. S. Binkley, D. J. Defrees, J. Baker, J. P. Stewart, M. Head-Gordon, C. Gonzalez, J. A. Pople, *Gaussian 94, Revision D.1*, Gaussian, Pittsburgh, PA, **1995**; b) M. J. Frisch, J. B. Foresman, *Gaussian 94 User's Reference*, Gaussian, Pittsburgh, PA, **1994–1996**.
- [9] J. J. P. Stewart, *J. Comput. Chem.* **1989**, *10*, 209–220.
- [10] W. J. Hehre, L. Radom, P. v. R. Schleyer, J. A. Pople, *Ab Initio Molecular Orbital Theory*, Wiley, New York, **1986**.
- [11] a) C. Lee, W. Yang, R. G. Parr, *Phys. Rev. B* **1988**, *37*, 785–789; b) A. D. Becke, *J. Chem. Phys.* **1993**, *98*, 5648–5652.
- [12] a) J. Tomasi, M. Persico, *Chem. Rev.* **1994**, *94*, 2027–2094; b) B. Ya. Simkin, I. Sheikhet, *Quantum Chemical and Statistical Theory of Solutions—A Computational Approach*, Ellis Horwood, London, **1995**, pp. 78–101.
- [13] a) M. W. Wong, M. J. Frisch, K. B. Wiberg, *J. Am. Chem. Soc.* **1991**, *113*, 4776–4782; b) M. W. Wong, K. B. Wiberg, M. J. Frisch, *J. Chem. Phys.* **1991**, *95*, 8991–8998.
- [14] a) M. J. S. Dewar, *Molecular Orbital Theory for Organic Chemists*, McGraw-Hill, New York, **1969**; b) K. Fukui, *Acc. Chem. Res.* **1971**, *4*, 57–64; c) I. Fleming, *Frontier Orbitals and Organic Chemical Reactions*, Wiley, New York, **1976**, chapter 2, pp. 5–32.
- [15] a) R. Sustmann, *Tetrahedron Lett.* **1971**, 2717–2720; b) R. Sustmann, *Tetrahedron Lett.* **1971**, 2721–2724.
- [16] For recent theoretical calculations on hetero-Diels–Alder reactions: a) R. Augusti, F. C. Gozzo, L. A. B. Moraes, R. Sparrapan, M. N. Eberlin, *J. Org. Chem.* **1998**, *63*, 4889–4897; b) T. M. V. D. Pinho e Melo, R. Fausto, A. M. A. Rocha Gonsalves, T. L. Gilchrist, *J. Org. Chem.* **1998**, *63*, 5350–5355; c) J. S. Chen, K. N. Houk, C. S. Foote, *J. Am. Chem. Soc.* **1998**, *120*, 12303–12309; d) T. Fernández, D. Suárez, J. A. Sordo, F. Monnat, E. Roversi, A. Estrella de Castro, K. Schenk, P. Vogel, *J. Org. Chem.* **1998**, *63*, 9490–9499.
- [17] *The Anomeric Effect and Associated Stereoelectronic Effects* (Ed.: G. R. J. Thatcher), American Chemical Society, Washington, DC, **1993**.
- [18] D. L. Boger, W. L. Corbett, T. T. Curran, A. M. Kasper, *J. Am. Chem. Soc.* **1991**, *113*, 1713–1729.
- [19] J. Liu, S. Niwayama, Y. You, K. N. Houk, *J. Org. Chem.* **1998**, *63*, 1064–1073.

- [20] Spectroscopic data for compound **11**:  $^1\text{H}$  NMR (400 MHz):  $\delta = 6.26$  (d,  $J_{9a,3a} = 5.3$  Hz, 1H; H9a), 5.39–5.36 (m, 2H; H1'', H2''), 5.25 (m, 1H; H4''), 5.15 (dd,  $J_{3',4'} = 1.9$  Hz,  $J_{3',2'} = 9.7$  Hz, 1H; H3''), 4.77 (t,  $J_{5,6} = J_{5',6'} = 6.0$  Hz, 1H; H6), 4.35 (dd,  $J_{5a',4'} = 4.2$  Hz,  $J_{5a',5b'} = 11.8$  Hz, 1H; H5a''), 4.05 (t, 1H; H2), 3.95 (m, 1H; CH<sub>3</sub>CH<sub>2</sub>O–C6), 3.85–3.76 (m, 2H; H5b'', H2''), 3.49 (m, 1H; CH<sub>3</sub>CH<sub>2</sub>O–C6), 3.19 (t,  $J_{3b,3a} = J_{3b,4} = 6.3$  Hz, 1H; H3b), 2.84 (m, 1H; H3a), 2.14 (s, 3H; OAc), 2.12 (s, 6H; 2 OAc), 2.09 (s, 3H; OAc), 2.02 (s, 3H; OAc), 2.12–1.93 (m, 3H; H4, H5, H3), 1.74 (m, 1H; H5'), 1.59 (m, 1H; H3'), 1.26 (t, 3H; CH<sub>3</sub>CH<sub>2</sub>O–C6);  $^{13}\text{C}$  NMR (100 MHz):  $\delta = 170.48$ , 170.37, 170.40 (5 OAc), 114.58 (C9a), 98.79 (C6), 74.37 (C3b), 71.95 (C4''), 67.84 (C1'', C2'', C3''), 67.27 (C2), 63.35 (CH<sub>3</sub>CH<sub>2</sub>O–C6), 62.57 (C5''), 48.37 (C4), 37.84 (C3a), 30.71 (C5), 27.32 (C3), 21.21, 20.76, 20.70, 20.65 (5 OAc), 15.07 (CH<sub>3</sub>CH<sub>2</sub>O).
- [21] a) For a concise review of solvent effects on the Diels–Alder reactions see: C. Catiuela, J. I. García, J. A. Mayoral, L. Salvatella, *Chem. Soc. Rev.* **1996**, 25, 209–218; b) W. Blokzijl, J. B. F. N. Engberts, in *Structure and Reactivity in Aqueous Solution. Characterization of Chemical and Biological Systems* (Eds.: C. J. Cramer, D. G. Truhlar), American Chemical Society, Washington, DC, **1994**, pp. 303–317.
- [22] C. Reichardt, *Solvent and Solvent Effects in Organic Chemistry*, VCH, Weinheim, **1990**, pp. 408–411.
- [23] a) H. Labaziewicz, F. G. Riddell, *J. Chem. Soc. Perkin Trans. 1* **1979**, 2926–2929; b) J. E. Baldwin, M. Otsuka, P. M. Wallace, *J. Chem. Soc. Chem. Commun.* **1985**, 1549–1550; c) M. Saburi, G. Kresze, H. Braun, *Tetrahedron Lett.* **1984**, 25, 5377–5380; d) H. Felber, G. Kresze, R. Prewo, A. Vasella, *Helv. Chim. Acta* **1986**, 69, 1137–1146.
- [24] a) J. J. Tufariello, in *1,3-Dipolar Cycloaddition Chemistry, Vol. 2* (Ed.: A. Padwa), Wiley, New York, **1984**, pp. 83–168; b) K. N. Houk, K. Yamaguchi in *1,3-Dipolar Cycloaddition Chemistry, Vol. 2* (Ed.: A. Padwa), Wiley, New York, **1984**, pp. 407–450; c) P. N. Confalone, E. M. Huie, *Org. React.* **1988**, 36, 1–173; d) E. Breuer, H. G. Aurich, A. Nielsen, *Nitrones, Nitronates and Nitroxides*, Wiley, Chichester, **1989**, pp. 1–104.
- [25] S. E. Denmark, M. Seierstad, B. Herbert, *J. Org. Chem.* **1999**, 64, 884–901.
- [26] a) A. Vasella, *Helv. Chim. Acta* **1977**, 60, 426–446; b) A. Vasella, *Helv. Chim. Acta* **1977**, 60, 1273–1295; c) For 1,3-dipolar cycloadditions with glycosyl nitrones see: L. Fisera, U. A. R. Al-Timari, P. Ertl, in *Cycloaddition Reactions in Carbohydrate Chemistry* (Ed.: R. M. Giuliano), American Chemical Society, Washington, DC, **1992**, pp. 158–171; stereocontrolled additions of sugar nitrones to organometallic nucleophiles have also been reported, see for instance: d) A. Dondoni, S. Franco, F. Junquera, F. L. Merchán, P. Merino, T. Tejero, V. Bertolasi, *Chem. Eur. J.* **1995**, 1, 505–520; e) A. Dondoni, F. Junquera, F. L. Merchán, P. Merino, M.-C. Scherrmann, T. Tejero, *J. Org. Chem.* **1997**, 62, 5484–5496.
- [27] S. Saito, T. Ishikawa, *Synlett* **1994**, 279–281.
- [28] a) S. Saito, T. Ishikawa, N. Kishimoto, T. Kohara, T. Moriwake, *Synlett* **1994**, 282–284; b) S. Saito, T. Ishikawa, T. Moriwake, *J. Org. Chem.* **1994**, 59, 4375–4377; c) T. Ishikawa, Y. Tajima, M. Fukui, S. Saito, *Angew. Chem.* **1996**, 108, 1990–1991; *Angew. Chem. Int. Ed. Engl.* **1996**, 35, 1863–1864.
- [29] T. K. M. Shing, Y.-L. Zhong, T. C. W. Mak, R.-J. Wang, F. Xue, *J. Org. Chem.* **1998**, 63, 414–415.
- [30] A. F. Bochkov, G. E. Zaikov, *Chemistry of the O-Glycosidic Bond: Formation and Cleavage*, Pergamon, Oxford, **1979**.
- [31] The reaction was conducted in methanol at room temperature for a week and monitored by  $^1\text{H}$  NMR (400 MHz).

Received: March 24, 1999 [F 1694]